

# NUMERICAL SIMULATION STUDY ON THE MECHANICAL CHARACTERISTICS OF DOWNHOLE HEAT FLUID GENERATORS IN HEAVY OIL THERMAL RECOVERY WELLS

by

**Wei MEI<sup>a,\*</sup>, Shanshan LIN<sup>a</sup>, Yubao SUN<sup>a</sup>, Weihang ZHANG<sup>a</sup>, Hongzhi SONG<sup>a</sup>,**

**Chunyue TONG<sup>a</sup>, Qingtao WANG<sup>a</sup>, Chang LIU<sup>a</sup>, Hongchuan ZHAO<sup>b</sup>**

<sup>a</sup>China National Offshore Oil Corporation China Ltd, China Oilfield Services Limited, Tianjin 300459, China

<sup>b</sup>MOE Key Laboratory of Petroleum Engineering, China University of Petroleum(Beijing), 102249, Beijing, China

*In this study, we conducted temperature, pressure, and stress deformation calculations for the tubing of a specific heavy oil thermal recovery well. Subsequently, we used the axial force on the tubing at the depth of the thermal fluid generator as a boundary condition and incorporated it into numerical simulation software to analyze the thermo-fluid-solid coupled mechanical characteristics of the generator under these operating conditions. Our findings indicate that the cooling water within the generator effectively isolates radial heat transfer from the thermal fluid. Moreover, under steam injection conditions, the maximum von-Mises stress in the generator is concentrated at the head-shell weld.*

*Keywords: heavy oil; thermal recovery well; thermal fluid generator; mechanical behavior; thermo-fluid-solid coupling*

## Introduction

Currently, the multi-phase thermal fluid techniques have emerged as a promising approach for heavy oil reservoir development due to their rapid effectiveness, ease of control, and operational flexibility. However, this technique faces challenges such as large land footprint, significant heat loss, and low thermal efficiency, making it economically challenging for offshore oil field development. Through extensive research, analysis, and proactive exploration, the use of downhole heat fluid generators as heating equipment during thermal recovery has been considered. Given the complex environment downhole, heat fluid generators are subjected to complex loads, including high temperatures and pressures. Therefore, it is essential to analyze the mechanical characteristics of downhole heat fluid generators during the heating process and establish corresponding safety assessment and optimization design methods to ensure the smooth progress of the heating operation.

---

\* Corresponding author; e-mail: meiwei@cosl.com.cn

The harsh operating environment of the downhole tubing in heavy oil thermal recovery wells exhibits significant temperature-pressure coupling effects. Accurately calculating the temperature and pressure distribution within the wellbore is a prerequisite for the mechanical analysis of thermal fluid generators. Cullender [1] obtained a pressure distribution model at the bottom of the well under steady-state flow conditions using average temperature and deviation coefficients. Ramey [2] considered temperature as a function of well depth and time for single-phase incompressible liquids or single-phase ideal gases, analyzing temperature distribution patterns within the wellbore. Shi *et al.* [3] comprehensively considered the influence of temperature and pressure factors. They established a coupled temperature-pressure distribution prediction model based on the principles of momentum conservation, energy conservation, and mass transfer and heat transfer theory. Additionally, researchers like Shuang Johancsik *et al.* [4] developed the classical downhole tubing friction torque model, known as the "soft rope" model, simplifying downhole tubing as a rope without bending stiffness. Mitchell *et al.* [5] improved the model by considering the contact position between downhole drill string and the wellbore, resulting in a more comprehensive rigid bar model. Wang *et al.* [6] considered the comprehensive effects of temperature and pressure variations during testing, constraints at the ends of the drill string, and buckling friction. They established a model for analyzing the forces acting on the testing drill string and developed mechanical analysis software for completing the testing of deep high-temperature and high-pressure gas wells. These studies have provided valuable insights into the temperature distribution in wellbores during circulation, the coupling of temperature and pressure, and the mechanical behavior of production tubing in high-temperature and high-pressure environments.

This paper utilized the FLUENT and LS-DYNA finite element software to perform a thermal-fluid-solid coupling simulation of the downhole heat fluid generator under steam injection conditions, taking into account the temperature, pressure, and stress distribution as boundary conditions at the depth where the generator is located in the tubing.

### **Engineering Background**

The oil and gas resources in the Bohai Sea area, especially heavy oil, are abundant and challenging to extract economically due to their high density and viscosity. Traditional surface-based heat fluid generators face issues of space constraints and heat loss in offshore operations. In contrast, the proposed downhole heat fluid generator is an improved version that generates and directly injects heat fluid into the reservoir from underground, enhancing economic feasibility. This downhole generator is based on the theory of liquid combustion injection, producing thermal energy by burning a high-temperature mixture at a specific depth. During operation, air, fuel, and cooling water flow into the generator from the head, generating heat fluid that is injected directly into the reservoir. This innovation saves offshore platform space, reduces heat loss, and ensures the economic viability of offshore heavy oil fields.

### **Mechanical Analysis**

The analysis assumes steady-state fluid flow in the wellbore, with stable heat transfer to the wellbore wall. Non-steady-state heat transfer is considered between the wellbore wall and the reservoir. The temperature and pressure gradients inside the wellbore

can be expressed as follows [6]:

$$\frac{dp}{dx} = \left( \rho g \sin \theta + f \frac{\rho v^2}{2d} \right) / \left( \frac{\rho v^2}{p} - 1 \right)$$

and

$$c_p \frac{dT}{dx} = - \frac{2\pi r_{T0} K_e}{W [r_{T0} U_{T0} f(t) + K_e]} (T - T_{ei0} + g_G z \sin \theta) + c_p c_J \frac{dp}{dx} + \frac{v^2}{p} \frac{dp}{dx} + f \frac{v^2}{2d} - g \sin \theta \quad (1)$$

where  $\rho$  is the fluid density,  $v$  is the fluid velocity,  $x$  is the well depth,  $p$  is pressure,  $g$  is the acceleration of gravity,  $\theta$  is the angle between the axial direction and the horizontal direction of the string,  $f$  is the friction coefficient,  $d$  is the inner diameter of the string,  $W$  is the mass flow rate of fluid,  $c_p$  is the specific heat capacity of the fluid,  $K_e$  is the formation thermal conductivity,  $r_{T0}$  is the outer radius of the string,  $U_{T0}$  is the total heat transfer coefficient,  $c_J$  is the Joule-Thompson coefficient, and  $p$  is the pressure in the string.

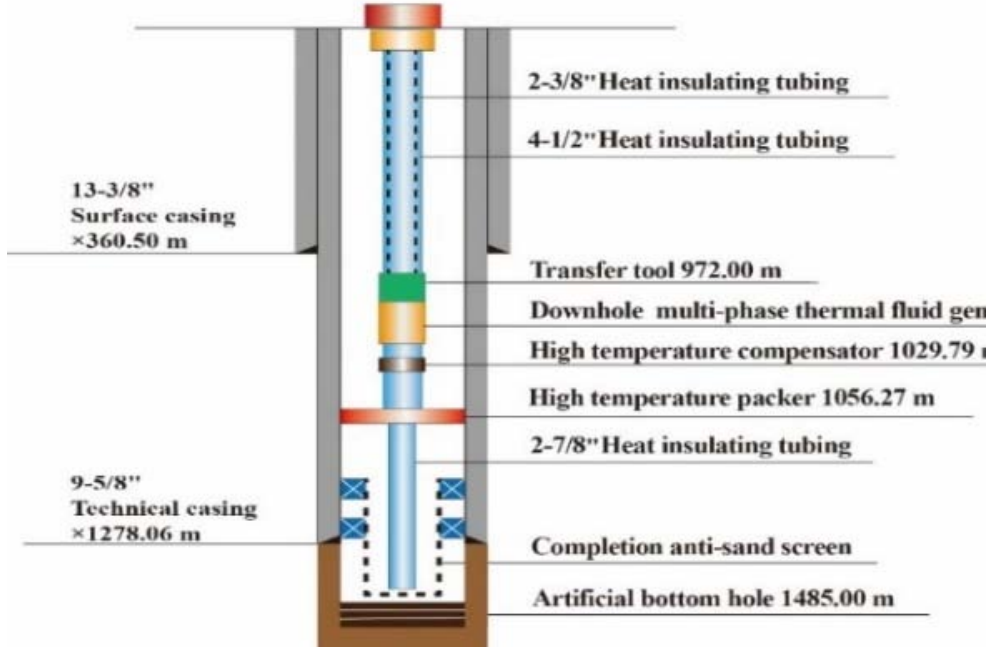


**Figure 1. Schematic diagram of integrated injection-production string**

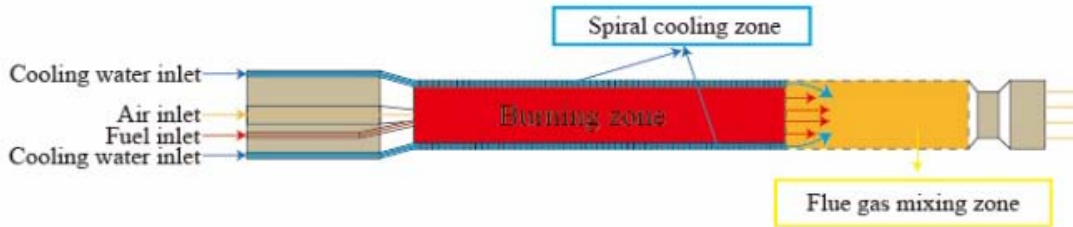


**Figure 2. Schematic Working principle diagram of heat fluid generator**

The integrated injection-production tubing structure is complex. To simplify the analysis of its axial stress and deformation, it is assumed that the cross-sectional area of the integrated injection-production tubing is always circular, the axis of the integrated injection-production tubing coincides with the wellbore axis, and the internal and external

pressures, gravity, and frictional resistance acting on the integrated injection-production tubing are uniformly distributed. The axial stress and deformation mechanical model of the insulating oil tube is shown in Figure 4.

The governing equation of the mechanical behavior can be written as [6]

$$\frac{\partial^2 u}{\partial s^2} = K_B \frac{\lambda \rho g \sin \alpha - \rho g \cos \alpha}{E} \quad (2)$$

subjected to The initial conditions and boundary conditions

$$u(0) = 0, EA_{tc} \frac{\partial u}{\partial s}(L) = -F \quad (3)$$

where  $u$  is the axial displacement,  $K_B$  is the buoyancy coefficient,  $\lambda = 0.25$ ,  $\alpha$  is the well inclination angle, and  $F_s$  is the setting force of the packer.

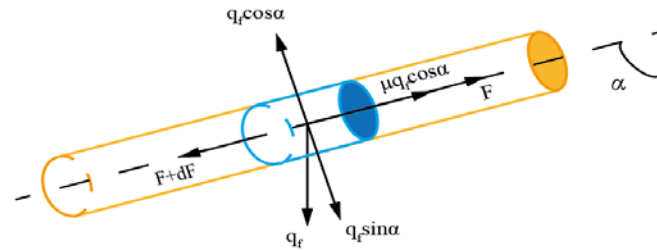


**Figure 4. Mechanical model of axial stress and deformation of tubing**

#### *Numerical Simulation of the Heat Fluid Generator*

The numerical simulation of the downhole heat fluid generator employs a thermal-fluid-solid coupling process. Initially, CFD software computes the combustion process to derive the combustion temperature field, which is subsequently mapped onto the generator structure. The temperature information, along with previously calculated axial forces in the tubing, is imported into LS-DYNA software for analyzing the mechanical characteristics of the generator. To address discrepancies in simulating combustion, the process involves calculating heat generation instead of directly simulating diesel combustion, followed by a simulation using a flow of carbon dioxide (CO<sub>2</sub>) at 1100°C as a substitute for diesel combustion products. There is

$$C_{12}H_{26} + 18.5O_2 = 12CO_2 + 13H_2O, Q = cm\Delta T \quad (4)$$

where  $Q$  is the energy released from diesel combustion,  $c$  is the specific heat capacity,  $m$  is the mass of the fluid, and  $\Delta T$  is the change in temperature.

#### **Case Analysis and Discussion**

##### *Calculation Data*

**Table1. Calculation parameters**

Parameter	Value	Parameter	Value
Diesel Calorific Value (MJ/kg)	42.6	Diesel Flow Rate (kg/s)	0.139
Carbon Dioxide Specific Heat Capacity (J/ (kg·K))	840	Water Specific Heat Capacity (J/ (kg·K))	4200
Initial Diesel Temperature (°C)	20	Turbulence Model	K-Omega
Structural Density (kg/m <sup>3</sup> )	8090	Thermal Fluid Inlet Velocity (kg/s)	2.0113
Thermal Fluid Inlet Temperature (°C)	1100	Cooling Water Inlet Velocity (kg/s)	2.361
Cooling Water Inlet Temperature (°C)	20	Thermal Conductivity	16.27

In this study, well X with a designed depth of 1485m is taken as an example. The

injection and production tubing string mainly consists of thermal insulation oil tubing, connecting tools, downhole thermal fluid generator, high-temperature bidirectional compensator, high-temperature deep well packer, etc. The thermal fluid generator is located at a depth of 975m in the well. The specific wellbore structure of this well is shown in Figure 6, and the remaining calculation parameters for this well are provided in Table 1.

## Calculation Results

### Wellbore Temperature and Pressure Distribution

Based on the analysis model constructed above, taking into account the compressibility of gas and the mutual coupling of temperature and pressure fields, and using parameters such as the formation thermal conductivity and geothermal gradient for this well, we have obtained the distribution patterns of the temperature and pressure fields along the entire wellbore, as shown in Figures 7 and 8.

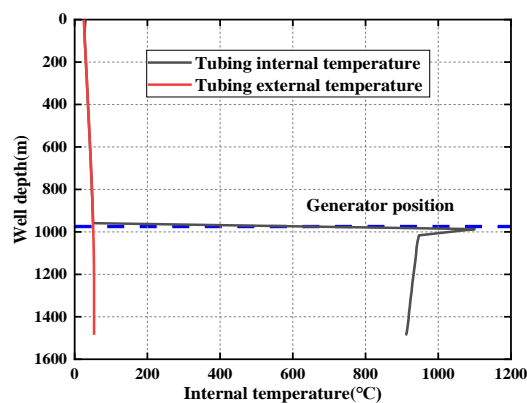


**Figure 5. Temperature distribution of the integrated injection-production string**

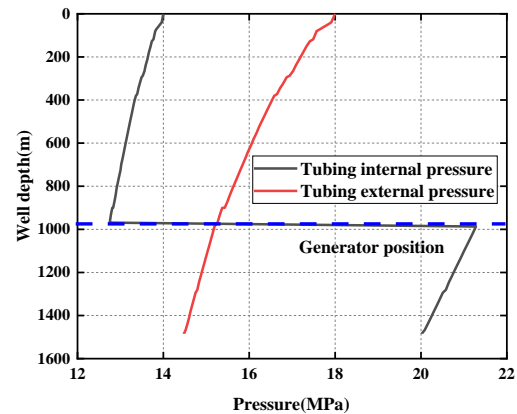


**Figure 6. Pressure distribution of the integrated injection-production string**

In Figure 5, under gas injection, tubing temperature varies from 30°C at the wellhead to a low of 27°C, then gradually increases to 51°C at the generator (975m). The generator heats it to 1100°C, followed by a decrease to 909°C at the well bottom. Outside the tubing, temperature rises from 25°C at the wellhead to 53°C at the well bottom. Notably, the presence of outer spiral grooves contributes to a significant temperature drop within the generator.

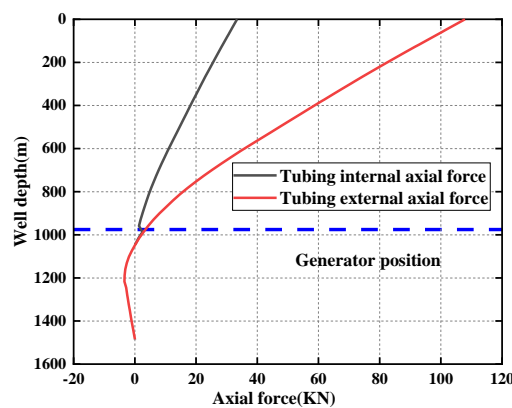


**Figure 7. Axial force distribution diagram of integrated injection-production string**

In Figure 6, the maximum internal pressure within the inner pipe column starts at 14 MPa at the wellhead, gradually decreasing to 12.75 MPa at the generator location. Passing through the generator, it spikes to 21.28 MPa due to fuel and oxidizer explosion, then

gradually decreases to 20 MPa. The external pressure of the outer pipe column decreases from 18 MPa at the wellhead to 14.48 MPa at the well bottom.

#### *Axial force distribution*

In Figure 7, under gas injection, the maximum axial tensile force in the inner oil pipe decreases from 33.4 kN at the wellhead to a minimum at the generator location. The outer oil pipe experiences a maximum axial tensile force of 107.8 kN at the wellhead and 3.5 kN at the generator. Beyond 1045m, the axial force becomes compressive, peaking at 3.5 kN before gradually decreasing to 0 kN.

#### *Analysis of temperature field calculation and generator mechanical stress*

Focusing on the internal combustion zone (Figure 8), the temperature within the generator's combustion zone consistently decreases from 1100°C to 947°C. Figure 9 shows the maximum von-Mises stress at the junction between the head and the shell, reaching approximately 114.5 MPa. Under combined temperature and mechanical loads, the generator elongates by 53.4 mm, with greater displacement closer to the right end.

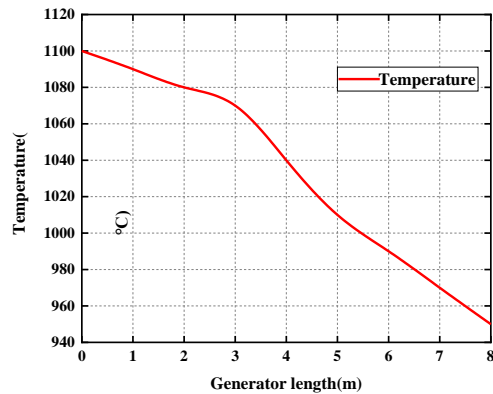


**Figure 8. Temperature distribution inside generator**

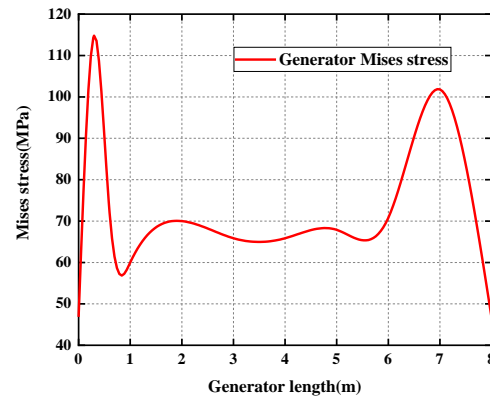


**Figure 9. von-Mises stress distribution diagram of generator**

Figure 10 shows the von-Mises stress distribution contour at the weld joint between the head and the shell of the generator (weld location), and Figure 11 displays the distribution of hoop stress at the weld root. The maximum von-Mises stress is 114.5 MPa, which does not exceed the yield limit of the material at this temperature (190 MPa). Therefore, the generator can safely operate under this condition.

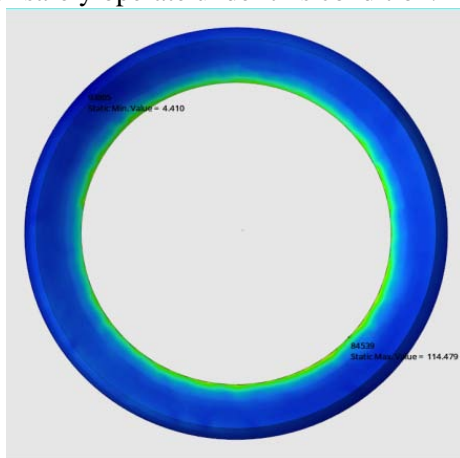


**Figure 10. von-Mises stress distribution diagram at key parts of generator**

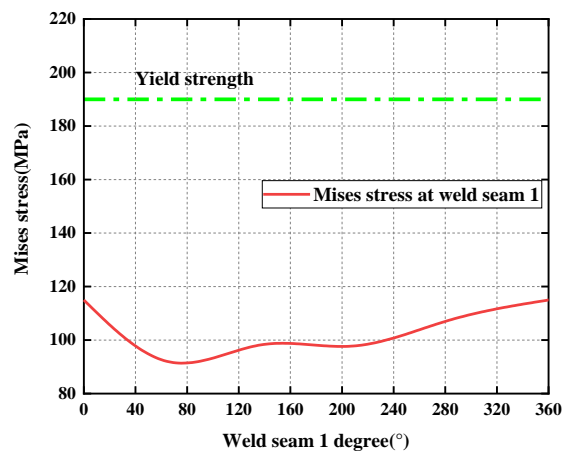


**Figure 11. von-Mises stress distribution diagram at key parts of generator**

## Generator Testing Process Design

The testing regime is determined based on injection rates of hot fluid and cooling water during steam injection. Simulations consider actual well conditions, exploring the generator's temperature field and structural stress distribution. Different injection rates for hot fluid and cooling water are tested, predicting the generator's stress, displacement, and temperature field distribution. See Table 2 for testing parameters.

**Table 2. Test parameters**

Types	Heat fluid injection velocity (kg/s)	Water injection velocity (kg/s)
Type1	3	2
Type2	4	2
Type3	4	3
Type4	4	4

### Displacement Distribution

In Figure 12, the generator's displacement increases along its length, peaking at 79 mm. Comparing Types 2, 3, and 4, higher cooling water injection rates reduce overall displacement, while higher hot fluid injection rates (Type 1 vs. Type 2) significantly increase displacement. In Figure 13, weld position 1 is identified as the critical area for von-Mises stresses, with the highest stress occurring there. Comparisons across test types indicate that increased cooling water injection rates decrease overall von-Mises stress, while higher hot fluid injection rates (Type 1 vs. Type 2) raise the generator's von-Mises stress levels.

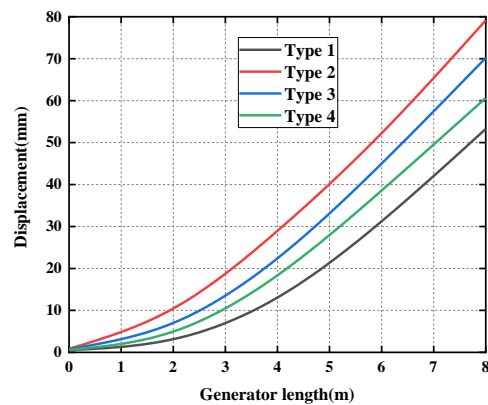


**Figure 12. Displacement distribution diagram of generator**

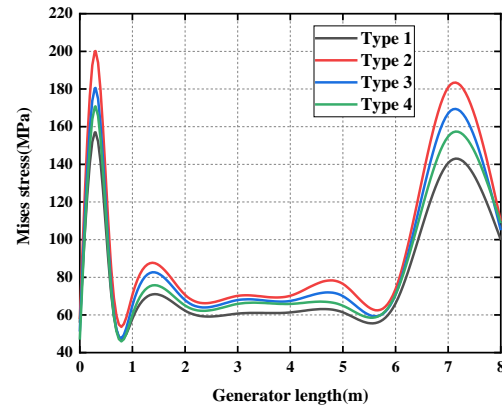


**Figure 13. von-Mises stress distribution diagram of hot fluid generator**

## Conclusions

Effective cooling water flow within the liner prevents the transfer of high temperatures from the combustion area to the outer tube of the generator, ensuring that the generator can operate in a relatively low-temperature environment, providing effective protection. The maximum von-Mises stress in the generator is located at the weld seam. It is advisable to avoid abrupt section changes and eliminate stress concentration phenomena. Additionally, the hot fluid injection rate should be kept below 4 kg/s.

## Nomenclature

$\rho$  -fluid density, [ kg/m<sup>3</sup>]

$x$  - well depth, [m]

$d$  -inner diameter of the string, [m]

$v$  -fluid velocity, [m/s]

$g$  -acceleration of gravity, [m/s<sup>2</sup>]

$W$  -the mass flow rate of fluid, [kg/s]

$c_p$ - specific heat capacity, [J/(kg·K)]	$K_e$ - thermal conductivity, [W/(m·K)]
$c_J$ -Joule-Thompson coefficient, [MPa/K]	$u$ - axial displacement, [m]
$\alpha$ -well inclination angle, [°]	$F_s$ -setting force of the packer, [N]
$Q$ -energy released from diesel combustion	$c$ -specific heat capacity, [J/(kg·K)]
$m$ -mass of the fluid, [kg]	$\Delta T$ -change in temperature, [°C]

### Acknowledgments

This research was funded by the scientific research projects of China National Offshore Oil Corporation China Ltd, China Oilfield Services Limited, Tianjin 300459, China; (Grant No. E-23227004).

### References

- [1] Cullender, M., *et al.*, Practical solution of gas-flow equations for wells and pipelines with large temperature gradients, *Transactions of the AIME*, 205(1956), 1, pp. 281-287
- [2] Ramey Jr, H. J., Wellbore heat transmission, *Journal of Petroleum Technology*, 14(1962), 4, pp. 427-435
- [3] Shi, X., *et al.*, Predictive analysis on borehole temperature and pressure of HTHP gas wells considering coupling effect, *Oil Drilling & Production Technology*, 4 (2018), 4, pp. 541-546
- [4] Johancsik, C., *et al.*, Torque and drag in directional wells-prediction and measurement, *Journal of Petroleum Technology*, 36(1984), 6, pp. 987–992
- [5] Mitchell, R., *et al.*, How good is the torque/drag model? *SPE Drilling & Completion*, 24(2009), 1, pp. 62-71
- [6] Wang, Y., *et al.*, Failure analysis of completion test string for deep high-temperature and high-pressure gas well: A Case Study on A Well in Shunnan Area, *Oil Drilling & Production Technology*, 44(2022), 2, pp. 302-308

Paper submitted: July 29, 2023

Paper revised: Doctor 23, 2023

Paper accepted: November 15, 2023